Hepatic protein tyrosine phosphatase 1B (PTP1B) deficiency protects against obesity-induced endothelial dysfunction

Abdelali Agouni[1,2], Simon Tual-Chalot[3,4], Matthieu Chalopin[3,4], Lucie Duluc[3,4], Nimesh Mody[1], M. Carmen Martinez[3,4,5], Ramaroson Andriantsitohaina[3,4,5*†] and Mirela Delibegović[1*†]

[1]University of Aberdeen, Institute of Medical Sciences, School of Medical Sciences, Foresterhill Health Campus, Aberdeen, AB25 2ZD, United Kingdom;
[2]University of Surrey, Faculty of Health and Medical Sciences, Department of Biochemistry and Physiology, Guildford, GU2 7XH, United Kingdom;
[3]LUNAM Université, Angers, France;
[4]INSERM U1063, Stress oxydant et pathologies métaboliques, Angers, France;
[5]CHU Angers, France
† Co-last authors

[*]Authors to whom correspondence should be addressed:
Dr Mirela Delibegović, University of Aberdeen, College of Life Sciences and Medicine, Institute of Medical Sciences, Aberdeen, AB25 2ZD, United Kingdom. Phone: +44 (0)1224 437587; E-mail: m.delibegovic@abdn.ac.uk

Dr Ramaroson Andriantsitohaina, INSERM, U1063, Stress oxydant et pathologies métaboliques, Université d'Angers, Rue des Capucins, Angers, F-49100, France. Phone: +33 (0)2 44 68 85 80, E-mail: ramaroson.andriantsitohaina@univ-angers.fr

Running Title: Liver-PTP1B deficiency protects against obesity-induced cardiovascular dysfunction.

Abstract

Growing evidence suggests that hepatic-insulin resistance is sufficient to promote progression to cardiovascular disease. We have shown previously that liver-specific protein-tyrosine-phosphatase 1B (PTP1B) deficiency improves hepatic-insulin sensitivity and whole-body glucose homeostasis. The aim of this study was to investigate the impact of liver-specific PTP1B-deficiency (L-PTP1B$^{-/-}$) on cardiac and peripheral vascular function, with special emphasis on endothelial function in the context of high-fat diet (HFD)-induced obesity.

L-PTP1B$^{-/-}$ mice exhibited an improved glucose and lipid homeostasis and increased insulin sensitivity, without changes in body weight. HFD-feeding increased systolic blood pressure (BP) in both L-PTP1B$^{-/-}$ and control littermates; however, this was significantly lower in L-PTP1B$^{-/-}$ mice. HFD-feeding increased diastolic BP in control mice only, whilst the L-PTP1B$^{-/-}$ mice were completely protected. The analysis of the function of the left ventricle (LV) revealed that HFD-feeding decreased LV fractional shortening in control animals, which was not observed in L-PTP1B$^{-/-}$ mice. Importantly, HFD feeding significantly impaired endothelium-dependent vasorelaxation in response to acetylcholine in aortas from control mice, whilst L-PTP1B$^{-/-}$ mice were fully protected. This was associated with alterations in eNOS phosphorylation. Selective inhibition of COX-2, using NS-398, decreased the contractile response in response to serotonin (5-HT) only in vessels from control mice. HFD-fed control mice released enhanced levels of prostaglandin E, a vasoconstrictor metabolite; whilst both chow- and HFD-fed L-PTP1B$^{-/-}$ mice released higher levels of prostacylin, a vasorelaxant metabolite.

Our data indicate that hepatic-PTP1B inhibition protects against HFD-induced endothelial dysfunction, underscoring the potential of peripheral PTP1B inhibitors in reduction of obesity-associated cardiovascular risk in addition to its anti-diabetic effects.

Introduction

Obesity incidence is reaching epidemic proportions worldwide, and is associated with an increased risk of premature death [1,2]. As a consequence, the incidence of obesity-related disorders, such as metabolic syndrome, diabetes and cardiovascular disease, is rising at an alarming rate. A common feature of these disorders is the development of insulin resistance, resulting in decreased insulin-stimulated glucose uptake, failure to suppress hepatic glucose production, and accumulation of hepatic lipids. Obesity, in particular abdominal obesity, was pointed out as a primary contributor to acquired insulin resistance, as increasing adiposity is correlated with impaired insulin action [1,3].

Growing evidence suggests that hepatic insulin resistance is sufficient to induce several components of the metabolic syndrome and promote progression to cardiovascular disease [1]. Vascular dysfunction related to obesity, in particular endothelial dysfunction in various vascular beds and in response to different vasodilator stimuli, might affect both peripheral vascular resistance and the delivery of substrates to metabolically active tissues, thereby contributing to both hypertension and metabolic abnormalities. Endothelial dysfunction is characterized by defects in the normal vasodilator response to mediators such as acetylcholine or to shear stress. It is considered as an independent predictor of cardiovascular events that has been consistently associated with obesity and the metabolic syndrome in a complex interplay with insulin resistance and inflammation. Deficiency of endothelial nitric oxide (NO) is believed to be the primary defect that links insulin resistance and endothelial dysfunction.

The mechanisms linking insulin resistance to endothelial dysfunction remain not well understood. There is evidence to suggest that the direct effects of insulin on the endothelium or disrupted endothelial insulin signalling may disturb endothelial function. Insulin stimulates endothelial cell production of NO [4], and, therefore, insulin resistance at the level of the endothelium might be expected to be associated with decreased insulin-stimulated NO. Duncan *et al.* [5] demonstrated that transgenic mice with endothelium-targeted over-expression of a dominant-negative mutant of human insulin receptor had a significant endothelial dysfunction, as evidenced by blunted aortic vasodilation in response to acetylcholine. The insulin receptor is a classic receptor tyrosine kinase and, as such, is inactivated by protein tyrosine phosphatases, notably the protein tyrosine phosphatase (PTP)1B [6]. PTP1B is also a negative regulator of leptin receptor signalling [7]. Whole-body PTP1B knockout studies in mice established PTP1B as a key negative regulator of body mass and insulin sensitivity. $PTP1B^{-/-}$ mice are lean, insulin sensitive, and have enhanced muscle

and liver insulin receptor phosphorylation [8,9]. Mice with brain-specific PTP1B$^{-/-}$ deficiency exhibit a similar phenotype to the global knockouts in terms of resistance to diet-induced obesity and enhanced insulin sensitivity, mostly due to central effect on leptin signalling [10]. Muscle-specific PTP1B deficient mice exhibit marked improvement in whole-body glucose homeostasis, without changes in body mass or adiposity as well as myeloid-cell specific knockouts [11]; whilst adipocyte-PTP1B deficient mice exhibit mild glucose intolerance and increased adipocyte cell size [12,13].

Liver-specific PTP1B deletion (L-PTP1B$^{-/-}$) improves whole-body glucose and lipid homeostasis, independently of changes in body mass/adiposity [14,15]. Liver-specific PTP1B$^{-/-}$ mice exhibit increased hepatic insulin signalling, enhanced insulin-induced suppression of hepatic glucose production in clamp studies and decreased expression of gluconeogenic genes. L-PTP1B$^{-/-}$ mice are also protected against HFD-induced increase in serum and liver triglyceride and cholesterol levels, associated with decreased expression of lipogenic genes [14,15]. Hepatic PTP1B may affect lipid metabolism via a pathway distinct from the insulin signalling where its location within the endoplasmic reticulum (ER) membrane appears critical. This was mainly attributable to L-PTP1B$^{-/-}$ mice being protected against obesity-induced ER stress in the liver [14,15]. ER stress has been reported to play a crucial role in insulin resistance and lipid accumulation [16].

Considering that *in vivo* liver-PTP1B deficiency improves hepatic insulin sensitivity and both global glucose homeostasis and lipid metabolism independently of changes in adiposity and body mass, we hypothesized that liver-specific PTP1B deficiency would also lead to protection against obesity-induced endothelial dysfunction and reduction of cardiovascular risk.

Experimental Procedures

Animal studies

All animal studies were performed under a project licence approved by the Home Office under the Animals (Scientific Procedures) Act 1986. Mice were maintained on a 12-hour light/dark cycle in a temperature-controlled barrier facility, with free access to water and food. L-PTP1B$^{-/-}$ mice were described previously and were achieved using an Albumin-cre promoter [14,15]. All mice studied were age-matched littermate males on the mixed 129Sv/C57Bl6 background. Genotyping for the PTP1B floxed allele and the presence of Albumin-Cre was performed by PCR [14,17]. Mice were placed either on standard chow pellet diet (Rat and Mouse Breeder and Grower, Special Diets Services, Horley, UK) or high-fat diet (HFD) (Adjusted Calories Diet, 55% Fat, Harlan Teklad, Belton, UK or Research Diets, 45% Fat) at weaning (21 days old), and weights were monitored weekly.

Metabolic measurements

Glucose from tail blood was assessed using a glucometer (Accu-Check, Burgess Hill, UK). Serum insulin was determined by ELISA (CrystalChem, Downers Grove, USA). Glucose tolerance tests (GTTs) were performed as described previously, following an overnight fast [12,14].

Blood Pressure

Each mouse was trained to the tail-cuff technique for 2 days before each measurement was recorded with a Physiograph Desk Model and an Electro-Sphygmomanometer (LE 5001 non-invasive blood pressure meter, Panlab, Barcelona, Spain). Five separate measurements were made on conscious mice for systolic and diastolic blood pressure (mmHg) and heart rate determinations.

Echocardiographic examination

In vivo transthoracic echocardiography was performed using a Vevo770 high frequency ultrasound machine (Visual Sonics, Toronto, Canada) in mice anesthetized with isoflurane (induction 5 %, maintenance 2 %) inhalation. Briefly, a two-dimensional short axis view of the left ventricle was obtained at the level of the papillary muscle in order to record M-mode tracings. Left ventricular end-diastolic diameter (LVEDD) and end-systolic diameter (LVESD) were measured by the American Society of Echocardiology leading-edge method from at least 3 consecutive cardiac cycles. Doppler cardiac output was calculated cardiac index was calculated by normalizing the cardiac output to the animal body weight as previously performed [18].

Vascular reactivity

Mice were sacrificed and aorta removed and carefully cleaned of adhering fat and connective tissue and then cut into rings (1.5-2 mm long) that were mounted on a wire myograph filled with physiological salt solution (PSS), as previously described [18-20]. Endothelium-dependent vasodilatation in response to acetylcholine (ACh, 1 nM to 10 µM, Sigma-Aldrich, St. Quentin, Fallavier, France) was studied in aortas with functional endothelium pre-contracted with the thromboxane A2 agonist (9, 11-dideoxy-11a, 9a-epoxymethanoprostaglandin F2-α) (U46619; Sigma-Aldrich, St. Quentin, Fallavier, France) at 80% of their maximal response in the presence or absence of the superoxide dismutase (SOD) mimetic, Mn(III)tetrakis(1-Methyl-4-pyridyl)porphyrin Pentachloride (MnTMPyP; Sigma-Aldrich, St. Quentin, Fallavier, France).

Contractile response was assessed by concentration-response curves by cumulative application of serotonin (5-HT, 1 nmol/ to 10 µmol/l; Sigma-Aldrich, St. Quentin, Fallavier, France) to aortas with functional endothelium in the absence or presence the given inhibitor pre-incubated for 30 min: the NO synthase inhibitor N^G-nitro-L-arginine (L-NA, 100 µmol/l; Sigma-Aldrich, St. Quentin, Fallavier, France), the selective cyclooxygenase (COX)-2 inhibitor N-(2-cyclohexyloxy-4-nitrophenyl) methanesulfonamide (NS-398, 10 µmol/l; Sigma-Aldrich, St. Quentin, Fallavier, France), indomethacin, the non-selective COX inhibitor (100 µmol/l; Sigma-Aldrich, St. Quentin, Fallavier, France). All inhibitors were used at maximal active concentrations at which they inhibit the release of either NO from all isoforms of NO synthases, metabolites from COX-2 isoform or metabolites from COX in blood vessels, as reported in many of our previous studies [18-20]. Higher concentrations of L-NA, NS-398 or indomethacin did not induce further inhibition.

Also, relaxation was assessed in response to sodium nitroprusside (SNP; Sigma-Aldrich, St. Quentin, Fallavier, France; 1 nM to 10 µM), a donor of NO in aorta rings pre-contracted with U46619.

Determination of prostanoid production

After sacrifice of mice, aorta was dissected and treated with 5-HT (1 µM, 37°C, 30 min; Sigma-Aldrich, St. Quentin, Fallavier, France) in 500 µL of PSS. After collection of the medium, prostacyclin, prostaglandin E and 8-isoprostane were measured by enzyme immunoassays kits (Cayman Chemicals, Ann Arbor, USA). The concentration of prostanoids was expressed as pg/ml/mg tissue (dry weight) [19].

Immunoblotting

Tissue lysates were prepared in radioimmunoprecipitation assay (RIPA) buffer as previously described [10,12,14]. Proteins were separated by 10% SDS-PAGE and transferred to

nitrocellulose membranes. Immunoblots were performed using antibodies against p-eNOS Ser 1177, p-eNOS Thr 495 (Cell Signaling Technology, Beverly, USA), COX-1, COX-2, eNOS, iNOS, caveolin-1 (BD Biosciences, San Jose, USA), Cu/Zn-SOD, Mn-SOD, EC-SOD (Stressgen Biotechnologies; Victoria, Canada), SHP-2 (Santa Cruz Biotechnology, Dallas, USA) and PTP1B (Abcam, Cambridge, UK). Immunoblots were developed with horseradish peroxidase-conjugated secondary antibody, visualized using enhanced chemiluminescence, and quantified by densitometry scanning.

superoxide anion (O_2^-) determination by electron paramagnetic resonance (EPR)

For superoxide anion (O_2^-) spin-trapping, mouse aortas were dissected and allowed to equilibrate in deferoxamine-chelated Krebs-Hepes solution containing 1-hydroxy-3methoxycarbonyl-2,2,5,5-tetramethylpyrrolidin (CMH, Noxygen; Denzlingen, Germany) (500 µM), deferoxamin (25 µM, Sigma-Aldrich, St. Quentin, Fallavier, France) and DETC (5 µM, Sigma-Aldrich, St. Quentin, Fallavier, France) under constant temperature (37°C) for 60 minutes. Then, they were frozen in liquid N_2 and analyzed in a Dewar flask by EPR. Values are expressed in unit/mg weight of dried tissue [18,19].

Data analysis

Data are expressed as mean ± SEM, and *n* represents the number of mice or biological replicates. Statistical analyses were performed using ANOVA (2-way or 1-way, as appropriate), and Mann-Whitney U tests. $P < 0.05$ was considered to be statistically significant.

Results

In vivo liver-PTP1B deficiency improves glucose and lipid homeostasis

As expected from our previous findings, this cohort of L-PTP1B$^{-/-}$ mice exhibited ~80% decrease in PTP1B protein in whole liver lysates compared to control littermates (Figure 1A). However, aortas from L-PTP1B$^{-/-}$ and control (fl/fl) mice expressed PTP1B to the same level (Figure 1A).

L-PTP1B$^{-/-}$ and control mice were weaned either onto normal chow diet (4.5% fat) or HFD (55% kcal from fat). There were no differences in body weight between the control and L-PTP1B$^{-/-}$ mice on either diet (Figure 1B) and as previously published [14]. There was a tendency for L-PTP1B$^{-/-}$ mice to have a slightly higher body mass, but this was not significant at any point. HFD-feeding increased to the same extent liver weight (Figure 1C) in both L-PTP1B$^{-/-}$ and control mice, but did not affect heart weight in either genotype (Figure 1D).

To assess the efficiency of HFD to induce glucose intolerance, we performed longitudinal glucose tolerance tests (GTTs). As expected, HFD-fed control mice developed glucose intolerance in a time-dependent manner (Figure 1E and 1F), whilst L-PTP1B$^{-/-}$ mice exhibited an enhanced ability to clear glucose from the peripheral circulation during intraperitoneal GTTs (at both 5- and 12-weeks of HFD) (Figure 1E and 1F).

By monitoring fasting glucose levels of L-PTP1B$^{-/-}$ and control littermates on HFD longitudinally, we determined that whilst at 5 weeks of HFD there were no differences in fasting glucose levels between the two groups, at 8 and 12 weeks of HFD-feeding control littermates developed fasting hyperglycemia (Figure 1G).

L-PTP1B$^{-/-}$ mice had markedly lower circulating insulin levels (Figure 1H), under both chow- and HFD-feeding conditions. This was associated with an increase in serum cholesterol levels upon HFD-feeding in control mice only, whilst L-PTP1B$^{-/-}$ mice had the same cholesterol levels as chow-fed mice (Figure 1I).

Collectively, these data indicate that, L-PTP1B$^{-/-}$ mice are protected against HFD-induced glucose intolerance and show improvements in lipid maintenance compared to their control littermates, like previously shown by us [14].

Liver-PTP1B deficiency protects against HFD-induced blood pressure increase and cardiac function alterations

Obesity is associated with hypertension and risk of developing cardiovascular disease [1,3,21]. To investigate the cardiovascular effects of liver-specific PTP1B deficiency in the context of obesity, blood pressure (BP) was monitored longitudinally in chow- and HFD-fed mice of both genotypes, using the non-invasive tail-cuff system. Prior to the terminal procedure, we performed the analysis of cardiac structure and function.

Heart rate was unaffected by short-term (3 weeks) or long-term (10 and 14 weeks) HFD-feeding in either genotype (Figure 2A). Short-term HFD-feeding (3 weeks) did not affect systolic blood pressure in either group; however, longer-term HFD-feeding (10- and 14-weeks) increased BP in both L-PTP1B$^{-/-}$ and control littermates; however, L-PTP1B$^{-/-}$ mice had significantly lower systolic BP compared to controls at both of these time-points (Figure 2B).

Diastolic BP was comparable between the groups for the first 10 weeks of HFD-feeding; however, whilst diastolic BP increased in the control fl/fl mice at 14 weeks post-HFD feeding, L-PTP1B$^{-/-}$ mice were protected (Figure 2C).

Next, we investigated by echocardiography the structure and function of the left ventricle of HFD-fed control and L-PTP1B$^{-/-}$ mice and compared it to their lean chow-fed respective controls. HFD-feeding increased systolic left-ventricular dimension (LVDs) in control fl/fl mice (Figure 2D), without affecting their diastolic left-ventricular dimension (LVDd) (Figure 2E). Interestingly however, HFD-feeding did not cause cardiac remodeling in L-PTP1B$^{-/-}$ mice, as measured by LVDs and LVDd (Figure 2D and 2E). Moreover, HFD-feeding decreased cardiac index in control fl/fl mice only, whilst L-PTP1B$^{-/-}$ remained completely protected (Figure 2F).

Liver-PTP1B deficiency protects against obesity-induced endothelial dysfunction in mouse aorta

Endothelial dysfunction, a key early factor in the development of atherosclerosis and a predictor of cardiovascular events, has been found in patients with obesity and metabolic syndrome [20]. Thus, the effect of liver-PTP1B deficiency on endothelial function was evaluated in aortas isolated from mice fed chow or HFD. On chow diet, there were no differences between the L-PTP1B$^{-/-}$ and control littermates (Figure 3A). As expected, HFD-feeding significantly impaired endothelium-dependent vaso-relaxation in response to acetylcholine in aortas collected from control fl/fl mice compared to chow diet-fed control fl/fl mice (Figure 3B). Remarkably, L-PTP1B$^{-/-}$ mice were completely protected against

HFD-induced endothelial dysfunction and remained as sensitive as chow-fed mice (Figure 3C).

To examine if the observed impaired response to acetylcholine in HFD-fed mice may be due to an impaired capacity of smooth muscle to dilate, the relaxation to an NO donor, SNP, was assessed in aortas from HFD-fed control fl/fl and L-PTP1B$^{-/-}$ mice. As shown in Figure 3D, response to SNP stimulation was similar in aortas from both control fl/fl and L-PTP1B$^{-/-}$ mice, indicating the absence of alterations in the capacity of smooth muscle to dilate.

Western blotting analyses demonstrated that HFD-feeding decreased eNOS phosphorylation at the activator site (Ser 1177) in aortas from both control fl/fl and L-PTP1B$^{-/-}$ mice, but eNOS phosphorylation was significantly higher in aortas from L-PTP1B$^{-/-}$ mice (Figure 4A). In addition, HFD-feeding enhanced, to the same extent, eNOS phosphorylation at the inhibitory site (Thr 495) in aortas from both control fl/fl and L-PTP1B$^{-/-}$ mice (Figure 4B), without affecting total eNOS (Figure 4C), caveolin-1 (Figure 4D) or iNOS (Figure 4E) levels.

Involvement of oxidative stress in HFD-induced endothelial dysfunction

Endothelial dysfunction is associated with oxidative stress [22]. To assess whether the protective effect of liver-PTP1B deletion on endothelial function involves a decrease in reactive oxygen species (ROS), the endothelium-dependent relaxation in response to acetylcholine was evaluated in aortas from HFD-fed control fl/fl and L-PTP1B$^{-/-}$ mice in the presence of the cell-permeant SOD mimetic, MnTMPyP, to blunt superoxide anion (O_2^-) production, the major ROS in vasculature.

Even in the presence of MnTMPyP, the endothelial dysfunction still persisted in vessels from control fl/fl mice only (Figure 5A), indicating that ROS may not be involved in the mechanism of protection in L-PTP1B$^{-/-}$ mice.

This was further confirmed by the absence of differences in O_2^- production in aortas from all groups (Figure 5B). Assessment of protein levels of the different isoforms of antioxidant SOD enzyme (Mn-, EC-, and Cu/Zn-SOD) demonstrated that Mn- and EC-SODs levels were not affected, whilst Cu/Zn-SOD was increased in aortas from PTP1B$^{-/-}$ mice under HFD condition (Figure 5C-5E).

Enhanced release of COX-derived vasodilators in aortas from L-PTP1B$^{-/-}$ mice

Vascular inflammation is reported to play a key role in obesity-induced vascular dysfunction [23]. Thus, the impact of HFD-feeding on vascular reactivity in response to vasoconstrictor agents was investigated with special emphasis on the relative contribution of inflammatory COX-derived agents in the regulation of vascular tone in both control fl/fl and L-PTP1B$^{-/-}$ mice, fed chow or HFD.

Concentration-response curves in response to serotonin (5-HT) were constructed in aortas from control fl/fl and L-PTP1B$^{-/-}$ mice in the presence or absence of COX inhibitors. In the absence of any inhibitor, aortas from HFD-fed mice displayed a trend towards enhanced response to 5-HT compared to those examined from chow-fed groups (Figure 6A). The non-selective inhibition of COX isoforms by indomethacin blunted, to the same extent, the contractile response to 5-HT in aortas from all the groups (Figure 6B). Interestingly, however, the selective inhibition of COX-2 isoform, achieved using NS-398, decreased contractile response only in vessels from control fl/fl mice whilst the latter was preserved in vessels obtained from L-PTP1B$^{-/-}$ mice (Figure 6C). This indicated either a presence of more COX-2-derived vasoconstrictor agents in control fl/fl mice and/or secretion of more COX-2-derived vasodilator agents in L-PTP1B$^{-/-}$ mice.

To investigate this, we analyzed COX-derived metabolite release from mouse aortas in all the experimental groups, which revealed that both chow- and HFD-fed L-PTP1B$^{-/-}$ mice exhibited higher levels of prostacylin, a vasodilator metabolite (Figure 6D). In addition, and as shown in Figure 6E, HFD-fed control fl/fl mice had higher levels of prostaglandin E, a vasoconstrictor metabolite, compared to chow–fed mice, whilst L-PTP1B$^{-/-}$ mice were completely protected.

The vasoconstrictor metabolite isoprostane-8 release was unaltered in all the groups (Figure 6F). Furthermore, these effects are independent of changes in COX-1 levels (Figure 6G and 6H); however, aortas from HFD-fed L-PTP1B$^{-/-}$ mice had increased protein levels of COX-2 (Figure 6G and 6I).

Discussion

We have previously shown that selectively deleting PTP1B in mouse liver results in improved glucose homeostasis and decreased levels of triglycerides and cholesterol, independently of changes in body weight or adiposity [14,24]. More recently, we also demonstrated that inflammatory ER-stress response and hepatic PTP1B expression are interlinked and that directly down-regulating PTP1B expression in liver can relieve over-activation of the ER-stress response associated with HFD-feeding, obesity and insulin resistance [15,16]. We now report that these improvements in hepatic insulin sensitivity in L-PTP1B$^{-/-}$ mice can also lead to a complete protection against obesity-induced endothelial dysfunction and cardiovascular remodelling, at least partly due to a further modulation of the relative contribution of COX-derived vasodilator agents in the regulation of vascular tone. Altogether, these studies show a complex interplay between obesity, hepatic insulin resistance and cardiovascular dysfunction and indicate that liver-PTP1B deficiency is able to improve several features of metabolic syndrome and thus highlight the potential utility of PTP1B inhibitors not only as anti-diabetic drugs but also as useful agents to protect against cardiovascular disease.

One of the major findings in the present work is that liver-PTP1B deletion protected mice *in vivo* against obesity-induced blood pressure increase and functional alterations of left ventricle, and improved glucose homeostasis at the same time. These data are consistent with observations in the literature associating impaired cardiac function with poor insulin sensitivity. Diabetes and insulin resistance often coexist with chronic heart failure in an inter-relationship such that each condition may impact on each other in terms of causation and outcome. In the Framingham study, Kannel *et al.* reported that nearly 20% of patients with chronic heart failure also had diabetes [25]. L-PTP1B$^{-/-}$ mice protection against HFD-induced increase in systolic and diastolic blood pressure and remodelling at the left ventricle level, was most likely due to the correction of peripheral insulin resistance in cardiac tissue. These findings are in line with a previous study from our group showing that treatment of Zucker fatty obese rats with red-wine polyphenol extract reduced glycaemia and blood pressure and improved left ventricle cardiac performances in obese rats [18]. Together with the current findings, these results reinforce the critical role of new insulin sensitizing approaches in correcting cardiac dysfunction associated with insulin resistance in cardiac tissue.

Other insulin sensitising strategies, however, were notable to correct cardiac alterations associated with insulin resistance. For instance, thiazolidinediones were reported to improve insulin sensitivity in the liver and peripheral tissues [26]; however, adverse

cardiovascular outcomes were also reported to be associated with the use of thiazolidinediones, most notably with chronic heart failure hospitalizations [27]. Liver-PTP1B targeting and its subsequent improvement of insulin sensitivity may lead to improved myocardial energy metabolism and thus to improved cardiac function [28]. Together these findings position the targeting of liver-PTP1B as a new and safe potential therapeutic approach to reduce both insulin resistance and cardiac disturbances associated to it.

Targeting directly PTP1B at the whole-body level either by genetic deletion in mouse or using pharmacological inhibitors was also shown to reduce adverse left ventricle remodelling, and to improve left ventricle function in a mouse model of chronic heart failure [29]. Nonetheless, because total PTP1B$^{-/-}$ mice are lean and resistant to obesity and dramatically insulin and leptin sensitive, and because of the systemic action of PTP1B inhibitors, it is very difficult to conclude from this study whether the observed effects are secondary to the global enhanced insulin sensitivity or a direct effect of PTP1B-deletion in the cardiovascular tree. The present findings suggest improvements in hepatic and global insulin sensitivity that can directly lead to an improvement in cardiac function in L-PTP1B$^{-/-}$ mice. These effects occur without affecting PTP1B in endothelial cells or cardiomyocytes and lead to protection against cardiovascular disease.

The present study showed that liver-PTP1B deletion was protective against obesity-induced endothelial dysfunction, an early step in development of atherosclerosis. Endothelial dysfunction was described to be inextricably associated with obesity and insulin resistance. Indeed, insulin receptors are present in endothelial cells and the disruption of endothelial insulin signalling may affect endothelial function [4,30]. At physiological concentrations, insulin stimulates both eNOS activity and expression in endothelial cells [31,32]. The phosphorylation of eNOS at Ser 1177 can be blunted by hyperglycaemia [33] and elevated concentrations of saturated free fatty acids under conditions of vascular insulin resistance [34]. In the present study, diet-induced obesity blunted the phosphorylation of eNOS at Ser 1177 in aortas from control mice while it was partially restored in vessels from L-PTP1B$^{-/-}$ mice most probably due to enhanced insulin sensitivity. Interestingly, the HFD-induced endothelial dysfunction was not associated with an increase in oxidative stress. In our study, mainly the contribution of superoxide anion was assessed, but other free radicals such as peroxynitrite may also play a role in the observed endothelial dysfunction [35]. It was shown that in HFD-fed L-PTP1B$^{-/-}$ mice, vascular Cu/Zn-SOD expression was increased while the superoxide production was not altered. These data may suggest that increased antioxidant defense mechanism participate to decrease oxidative stress in these animals. Thus

decrease and/or normalization of oxidative stress might be responsible for most of the cardiovascular protection in the current study.

Interestingly, aortas from HFD-fed L-PTP1B$^{-/-}$ had a fully preserved vasoconstrictor response to 5-HT in the presence of COX-inhibitors. This was associated with reduced levels of COX-derived vasoconstrictors (prostaglandin E) and enhanced production of vasodilators (prostacyclins) owing to an increase in COX-2 levels. The reduction in the secretion of prostacyclin together with NO by the endothelium forms the basis of endothelial abnormality in diabetes. Clinical and experimental diabetes are associated with a reduction in prostacyclin secretion [36,37]. The increased level of prostacyclin is thus a compensatory mechanism which may participate in maintaining endothelium-dependent relaxation within physiological range in aortas from L-PTP1B$^{-/-}$ mice. Consistent with the present findings, previous studies indicated that COX-2 protein levels are elevated in the aortas of mice with obesity and type 2 diabetes [38]. In addition, in diabetic patients, vascular expression of COX-2 was found to be markedly elevated in coronary arterioles and bradykinin induced enhanced COX-2-derived prostaglandin-mediated dilation in these vessels [39]. Furthermore, in L-PTP1B$^{-/-}$ mice, improved left ventricle function may lead to improved haemodynamics and thus participate in the improvement of endothelial function through for example an increase in vascular shear stress. It has previously been reported that insulin resistance decreases activity of arterial prostacyclin synthase, the key enzyme involved in prostanoid biosynthesis of prostacyclin, by increasing endothelial fatty acid oxidation [40]. Here, we report that liver-PTP1B deletion improved whole-body insulin resistance and lipid metabolism in addition to decreasing ER stress response, as previously reported by us [14,15]. Altogether, these effects may improve the activity of prostacyclin synthase thus leading to increased levels of vascular prostacylin release.

Several studies have reported that direct whole-body targeting of PTP1B improved endothelial function in different cardiovascular disease animal models of obesity and chronic heart failure [29,41,42]. Ali *et al.* [41] demonstrated that total PTP1B knock-down improved endothelial function in peripheral vessels from obese and diabetic leptin-receptor deficient *db/db* mice. Gomez *et al.* [29] and Vercauteren *et al.* [42] reported in mouse models of chronic heart failure that both genetic deletion and pharmacological inhibition of PTP1B improved flow-mediated dilation in small mesenteric arteries. However, these experimental models do not allow to distinghish whether this improvement is due to global enhancement of insulin sensitivity or due to PTP1B deletion in endothelial cells themselves because of the systemic targeting of PTP1B in these animals. Indeed, these findings may reflect a direct role

of PTP1B in the endothelium with special emphasis on eNOS activation and NO release, through enhanced tyrosine phosphorylation of eNOS. Activation of eNOS by shear stress was indeed shown to require tyrosine phosphorylation [43] in addition to the classical phosphorylation pattern on Ser 1177. The generation of endothelium-specific PTP1B knockouts will help addressing these conflicting mechanistic points.

Finally, inflammatory signalling was not assessed in the present study that may contribute to endothelial dysfunction. However, very recently, it has been reported that PTP1B deletion protects against septic-shock-induced cardiovascular function resulting from reduction of inflammation [44]. Such mechanism might be also implicated in the improvement of endothelial dysfunction reported here. Furthermore, we have previously shown that because of its critical localisation within the ER membrane liver-PTP1B deletion decreased ER stress response [14,15], which has been reported to play a crucial role in insulin resistance and lipid accumulation [16] and more recently was shown to play an important role in endothelial dysfunction in experimental models of diabetes and hypertension [45,46]. Diagram shown in Figure 7 summarizes the main mechanisms behind improved cardiovascular function in L-PTP1B$^{-/-}$ mice.

Altogether, our findings further demonstrate the critical role of PTP1B in hepatic glucose and lipid metabolism and underscore the importance of targeting liver-PTP1B as a strategy to reduce cardiovascular risk in the context of obesity and metabolic syndrome.

Acknowledgments

This work was supported by a Diabetes UK project grant to Dr M. Delibegović (BDARD08/0003597), Tenovus Scotland grant to Dr. M. Delibegovic and Dr. A. Agouni and travel grants from the Physiological Society and Company of Biologists to Dr. A. Agouni. Dr Delibegovic is also funded by an RCUK Fellowship, British Heart Foundation, EFSD/Lilly diabetes programme grant and the Royal Society. Dr Agouni is funded by the Royal Society and the Physiological Society. This work is supported by the INSERM and CHU of Angers. The authors are thankful to the functional imaging center of Angers (CIFAB) for the use of echocardiography.

Duality of interest: None to declare.

Figure Legends

Figure 1. *In vivo* liver-PTP1B deletion improves glucose and lipid homeostasis independently of body mass changes

(A) PTP1B protein levels in livers (n = 3) and aortas (n = 6) from fl/fl control and L-PTP1B$^{-/-}$ mice. **(B)**

Terminal body weights of fl/fl control and L-PTP1B$^{-/-}$ mice fed either chow or high fat diets. **(C)** Terminal liver weights from fl/fl control and L-PTP1B$^{-/-}$ mice fed either chow or high fat diets. **(D)** Terminal heart weights from fl/fl control and L-PTP1B$^{-/-}$ mice fed either chow or high fat diets. **(E)** GTTs in fl/fl control and L-PTP1B$^{-/-}$ mice at 5 weeks of HFD. **(F)** GTTs in fl/fl control and L-PTP1B$^{-/-}$ mice at 12 weeks of HFD. **(G)** Fasting blood glucose in fl/fl control and L-PTP1B$^{-/-}$ mice at 5, 8 and 12 weeks of HFD. **(H)** Fasting insulin levels in fl/fl control and L-PTP1B$^{-/-}$ mice fed either chow or high fat diets. **(I)** Total cholesterol circulating levels in fl/fl control and L-PTP1B$^{-/-}$ mice fed either chow or high fat diets. Data are presented as mean± SEM and were analysed by either by one-way or two-way (E, F) ANOVA or one-way ANOVA, followed with a Tukey's multiple comparison test. *P<0.05, **P<0.01, ***P<0.001 *vs.* the indicated group or chow fl/fl and $^{\#\#}$ P < 0.01 *vs.* chow L-PTP1B$^{-/-}$ (n = 7-11 in each group).

Figure 2. Liver-PTP1B deletion protects against obesity-induced blood pressure increase and cardiac function alterations

(A) Heart rate in fl/fl control and L-PTP1B$^{-/-}$ mice at 5, 10 and 14 weeks of HFD. **(B)** Systolic blood pressure in fl/fl control and L-PTP1B$^{-/-}$ mice at 5, 10 and 14 weeks of HFD. **(C)** Diastolic blood pressure in fl/fl control and L-PTP1B$^{-/-}$ mice at 5, 10 and 14 weeks of HFD. **(D)** End-Systolic left ventricle (LV) dimension in in fl/fl control and L-PTP1B$^{-/-}$ mice fed either chow or high fat diets. **(E)** End-Diastolic left ventricle (LV) dimension in in fl/fl control and L-PTP1B$^{-/-}$ mice fed either chow or high fat diets. **(F)** Cardiac index (CI) in fl/fl control and L-PTP1B$^{-/-}$ mice fed either chow or high fat diets. Data are presented as mean± SEM and were analysed by one-way ANOVA, followed with a Tukey's multiple comparison test. *P<0.05, ***P<0.001 *vs.* 3 weeks HFD or chow mice; $^{\#}$P<0.05 vs. fl/fl mice in the same group. (n = 7-11 in each group).

Figure 3. Liver-PTP1B deletion protects against obesity-induced endothelial dysfunction in mouse aorta

(A) Endothelium-dependent relaxation in response to ACh in aortas from fl/fl control and L-PTP1B$^{-/-}$ mice fed chow diet. **(B)** Endothelium-dependent relaxation in response to ACh in aortas from fl/fl control mice fed either chow or high fat diets. **(C)** Endothelium-dependent

relaxation in response to ACh in aortas from fl/fl control and L-PTP1B$^{-/-}$ mice fed HFD. **(D)** Endothelium-independent relaxation in response to SNP in aortas from fl/fl control and L-PTP1B$^{-/-}$ mice fed. Data are presented as mean± SEM and were analysed by two-way ANOVA. **P<0.01, ***P<0.001 *vs.* indicated group. (n = 7-11 in each group).

Figure 4. Altered eNOS signalling in mouse aorta from L-PTP1B$^{-/-}$ mice (A) Phosphorylation of eNOS on activator site Ser 1177 in aortas from fl/fl control and L-PTP1B$^{-/-}$ mice fed either chow or high fat diets. **(B)** Phosphorylation of eNOS on inhibitor site Thr 495 in aortas from fl/fl control and L-PTP1B$^{-/-}$ mice fed either chow or high fat diets. **(C)** Total eNOS expression in aortas from fl/fl control and L-PTP1B$^{-/-}$ mice fed either chow or high fat diets. **(D)** Caveolin-1 expression in aortas from fl/fl control and L-PTP1B$^{-/-}$ mice fed either chow or high fat diets. **(E)** iNOS expression in aortas from fl/fl control and L-PTP1B$^{-/-}$ mice fed either chow or high fat diets. Western blots results are representative of 3 independent experiments (n = 3 mice in each group), and the densitometry values are expressed in arbitrary units (A.U.). Data are presented as mean± SEM and were analysed by one-way ANOVA, followed with a Tukey's multiple comparison test. **P<0.01*vs.* chow groups and $^{\#}$P<0.05 vs. the indicated group.

Figure 5. Oxidative stress in not involved in obesity-induced endothelial dysfunction in mouse aorta

(A) Endothelium-dependent relaxation in response to ACh in the presence of SOD mimetic (MnTMPyP) in aortas from fl/fl control and L-PTP1B$^{-/-}$ mice fed HFD. **(B)** Superoxide anion (O_2^-) production in aortas from fl/fl control and L-PTP1B$^{-/-}$ mice fed either chow or high fat diets. Mn SOD **(C),** EC SOD SOD **(D)** and Cu/Zn **(E)** expressions in aortas from fl/fl control and L-PTP1B$^{-/-}$ mice fed either chow or high fat diets. Western blots results are representative of 3 independent experiments (n = 3 mice in each group), and the densitometry values are expressed in arbitrary units (A.U.). Data are presented as mean± SEM and were analysed either by two-way ANOVA (A) or one-way ANOVA, followed with a Tukey's multiple comparison test (B-E). *P<0.05*vs.* fl/fl mice.

Figure 6. Enhanced release of COX-2 derived vasodilators in aortas from L-PTP1B$^{-/-}$ mice

(A) Vascular reactivity in response to 5-HT agonist in aortas from fl/fl control and L-PTP1B$^{-/-}$ mice fed either chow or high fat diets. **(B)** Vascular reactivity in response to 5-HT agonist in the presence of non-selective COX inhibitor, indomethacin, in aortas from fl/fl control and L-PTP1B$^{-/-}$ mice fed either chow or high fat diets. **(C)** Vascular reactivity in response to 5-HT agonist in the presence of COX-2 selective inhibitor, NS398, in aortas from fl/fl control and

L-PTP1B$^{-/-}$ mice fed either chow or high fat diets. **(D)** Prostacyclin release in aortas from fl/fl control and L-PTP1B$^{-/-}$ mice fed either chow or high fat diets. **(E)** Prostaglandin E release in aortas from fl/fl control and L-PTP1B$^{-/-}$ mice fed either chow or high fat diets. **(F)** 8-Isoprostane release in aortas from fl/fl control and L-PTP1B$^{-/-}$ mice fed either chow or high fat diets. **(G)** COX-1 and COX-2 protein expressions in aortas from fl/fl control and L-PTP1B$^{-/-}$ mice fed either chow or high fat diets. Western blots results are representative of 3 independent experiments (n = 3 mice in each group), and the densitometry values are expressed in arbitrary units (A.U.). Data are presented as mean± SEM and were analysed either by or two-way ANOVA (A-C) or one-way ANOVA followed with a Tukey's multiple comparison test (D-H). *P<0.05, **P<0.01, ***P<0.001*vs.* the indicated group or fl/fl mice.

Figure 7. Summary of mechanisms involved in cardiovascular liver-PTP1B actions

Obesity leads to an increase in the expression and activity of PTP1B in the liver which will then cause hepatic insulin resistance through the inactivation of insulin receptor signalling pathway. Furthermore, because of its critical localisation within the endoplasmic reticulum (ER) membrane, PTP1B will also lead to activation of the ER stress response pathway, leading to lipid accumulation and activation of inflammatory pathways. Altogether, impaired hepatic glucose homeostasis and increased lipid metabolism in addition to ER stress activation will eventually cause endothelial dysfunction in peripheral vessels and impair cardiac function. These are normalised by hepatic PTP1B deficiency.

References

[1] Reaven G. Is insulin resistance: the link between TG-rich lipoproteins and excess death? J.Intern.Med. 2011;270:600,1; author reply 602-3.

[2] Sesti G. Pathophysiology of insulin resistance. Best Pract.Res.Clin.Endocrinol.Metab. 2006;20:665-79.

[3] Reaven GM. Relationships among insulin resistance, type 2 diabetes, essential hypertension, and cardiovascular disease: similarities and differences. J.Clin.Hypertens.(Greenwich) 2011;13:238-43.

[4] Zeng G, Nystrom FH, Ravichandran LV, Cong LN, Kirby M, Mostowski H, et al. Roles for insulin receptor, PI3-kinase, and Akt in insulin-signaling pathways related to production of nitric oxide in human vascular endothelial cells. Circulation 2000;101:1539-45.

[5] Duncan ER, Crossey PA, Walker S, Anilkumar N, Poston L, Douglas G, et al. Effect of endothelium-specific insulin resistance on endothelial function in vivo. Diabetes 2008;57:3307-14.

[6] Kopelman PG. Obesity as a medical problem. Nature 2000;404:635-43.

[7] Tsou RC, Bence KK. The Genetics of PTPN1 and Obesity: Insights from Mouse Models of Tissue-Specific PTP1B Deficiency. J.Obes. 2012;2012:926857.

[8] Elchebly M, Payette P, Michaliszyn E, Cromlish W, Collins S, Loy AL, et al. Increased insulin sensitivity and obesity resistance in mice lacking the protein tyrosine phosphatase-1B gene. Science 1999;283:1544-8.

[9] Klaman LD, Boss O, Peroni OD, Kim JK, Martino JL, Zabolotny JM, et al. Increased energy expenditure, decreased adiposity, and tissue-specific insulin sensitivity in protein-tyrosine phosphatase 1B-deficient mice. Mol.Cell.Biol. 2000;20:5479-89.

[10] Bence KK, Delibegovic M, Xue B, Gorgun CZ, Hotamisligil GS, Neel BG, et al. Neuronal PTP1B regulates body weight, adiposity and leptin action. Nat.Med. 2006;12:917-24.

[11] Grant L, Shearer KD, Czopek A, Lees EK, Owen C, Agouni A, et al. Myeloid-Cell Protein Tyrosine Phosphatase-1B Deficiency in Mice Protects Against High-Fat Diet and Lipopolysaccharide-Induced Inflammation, Hyperinsulinemia, and Endotoxemia Through an IL-10 STAT3-Dependent Mechanism. Diabetes 2014;63:456-70.

[12] Delibegovic M, Bence KK, Mody N, Hong EG, Ko HJ, Kim JK, et al. Improved glucose homeostasis in mice with muscle-specific deletion of protein-tyrosine phosphatase 1B. Mol.Cell.Biol. 2007;27:7727-34.

[13] Owen C, Czopek A, Agouni A, Grant L, Judson R, Lees EK, et al. Adipocyte-specific protein tyrosine phosphatase 1B deletion increases lipogenesis, adipocyte cell size and is a minor regulator of glucose homeostasis. PLoS One 2012;7:e32700.

[14] Delibegovic M, Zimmer D, Kauffman C, Rak K, Hong EG, Cho YR, et al. Liver-specific deletion of protein-tyrosine phosphatase 1B (PTP1B) improves metabolic syndrome and attenuates diet-induced endoplasmic reticulum stress. Diabetes 2009;58:590-9.

[15] Agouni A, Mody N, Owen C, Czopek AJ, Zimmer D, Bentires-Alj M, et al. Liver-specific deletion of protein tyrosine phosphatase (PTP) 1B improves obesity- and pharmacologically-induced endoplasmic reticulum stress. Biochem.J. 2011.

[16] Owen C, Lees EK, Grant L, Zimmer DJ, Mody N, Bence KK, et al. Inducible liver-specific knockdown of protein tyrosine phosphatase 1B improves glucose and lipid homeostasis in adult mice. Diabetologia 2013;56:2286-96.

[17] Bence KK. Hepatic PTP1B Deficiency: The Promise of a Treatment for Metabolic Syndrome? J.Clin.Metab.Diabetes 2010;1:27-33.

[18] Agouni A, Lagrue-Lak-Hal AH, Mostefai HA, Tesse A, Mulder P, Rouet P, et al. Red wine polyphenols prevent metabolic and cardiovascular alterations associated with obesity in Zucker fatty rats (Fa/Fa). PLoS One 2009;4:e5557.

[19] Agouni A, Ducluzeau PH, Benameur T, Faure S, Sladkova M, Duluc L, et al. Microparticles from patients with metabolic syndrome induce vascular hypo-reactivity via Fas/Fas-ligand pathway in mice. PLoS One 2011;6:e27809.

[20] Agouni A, Lagrue-Lak-Hal AH, Ducluzeau PH, Mostefai HA, Draunet-Busson C, Leftheriotis G, et al. Endothelial dysfunction caused by circulating microparticles from patients with metabolic syndrome. Am.J.Pathol. 2008;173:1210-9.

[21] Reaven GM. Insulin resistance: the link between obesity and cardiovascular disease. Med.Clin.North Am. 2011;95:875-92.

[22] Schulz E, Gori T, Munzel T. Oxidative stress and endothelial dysfunction in hypertension. Hypertens.Res. 2011;34:665-73.

[23] Taube A, Schlich R, Sell H, Eckardt K, Eckel J. Inflammation and metabolic dysfunction: links to cardiovascular diseases. Am.J.Physiol.Heart Circ.Physiol. 2012;302:H2148-65.

[24] Delibegovic M, Mody N. PTP1B in the Periphery: Regulating Insulin Sensitivity and ER Stress. In: Bence KK, editor. Protein Tyrosine Phosphatase Control of MetabolismNew York: Springer, 2013. p. 91-105.

[25] Kannel WB, Hjortland M, Castelli WP. Role of diabetes in congestive heart failure: the Framingham study. Am.J.Cardiol. 1974;34:29-34.

[26] Nissen SE, Nicholls SJ, Wolski K, Nesto R, Kupfer S, Perez A, et al. Comparison of pioglitazone vs glimepiride on progression of coronary atherosclerosis in patients with type 2 diabetes: the PERISCOPE randomized controlled trial. JAMA 2008;299:1561-73.

[27] Lago RM, Singh PP, Nesto RW. Congestive heart failure and cardiovascular death in patients with prediabetes and type 2 diabetes given thiazolidinediones: a meta-analysis of randomised clinical trials. Lancet 2007;370:1129-36.

[28] Belke DD, Betuing S, Tuttle MJ, Graveleau C, Young ME, Pham M, et al. Insulin signaling coordinately regulates cardiac size, metabolism, and contractile protein isoform expression. J.Clin.Invest. 2002;109:629-39.

[29] Gomez E, Vercauteren M, Kurtz B, Ouvrard-Pascaud A, Mulder P, Henry JP, et al. Reduction of heart failure by pharmacological inhibition or gene deletion of protein tyrosine phosphatase 1B. J.Mol.Cell.Cardiol. 2012;52:1257-64.

[30] Aljada A, Dandona P. Effect of insulin on human aortic endothelial nitric oxide synthase. Metabolism 2000;49:147-50.

[31] Kim JA, Montagnani M, Koh KK, Quon MJ. Reciprocal relationships between insulin resistance and endothelial dysfunction: molecular and pathophysiological mechanisms. Circulation 2006;113:1888-904.

[32] Kuboki K, Jiang ZY, Takahara N, Ha SW, Igarashi M, Yamauchi T, et al. Regulation of endothelial constitutive nitric oxide synthase gene expression in endothelial cells and in vivo : a specific vascular action of insulin. Circulation 2000;101:676-81.

[33] Federici M, Menghini R, Mauriello A, Hribal ML, Ferrelli F, Lauro D, et al. Insulin-dependent activation of endothelial nitric oxide synthase is impaired by O-linked glycosylation modification of signaling proteins in human coronary endothelial cells. Circulation 2002;106:466-72.

[34] Du X, Edelstein D, Obici S, Higham N, Zou MH, Brownlee M. Insulin resistance reduces arterial prostacyclin synthase and eNOS activities by increasing endothelial fatty acid oxidation. J.Clin.Invest. 2006;116:1071-80.

[35] Liaudet L, Vassalli G, Pacher P. Role of peroxynitrite in the redox regulation of cell signal transduction pathways. Front.Biosci.(Landmark Ed) 2009;14:4809-14.

[36] Hendra T, Betteridge DJ. Platelet function, platelet prostanoids and vascular prostacyclin in diabetes mellitus. Prostaglandins Leukot.Essent.Fatty Acids 1989;35:197-212.

[37] Shepherd GL, Lewis PJ, Blair IA, de Mey C, MacDermot J. Epoprostenol (prostacyclin, PGI2) binding and activation of adenylate cyclase in platelets of diabetic and control subjects. Br.J.Clin.Pharmacol. 1983;15:77-81.

[38] Guo Z, Su W, Allen S, Pang H, Daugherty A, Smart E, et al. COX-2 up-regulation and vascular smooth muscle contractile hyperreactivity in spontaneous diabetic db/db mice. Cardiovasc.Res. 2005;67:723-35.

[39] Szerafin T, Erdei N, Fulop T, Pasztor ET, Edes I, Koller A, et al. Increased cyclooxygenase-2 expression and prostaglandin-mediated dilation in coronary arterioles of patients with diabetes mellitus. Circ.Res. 2006;99:e12-7.

[40] Du X, Edelstein D, Obici S, Higham N, Zou MH, Brownlee M. Insulin resistance reduces arterial prostacyclin synthase and eNOS activities by increasing endothelial fatty acid oxidation. J Clin Invest. 2006;116:1071-80.

[41] Ali MI, Ketsawatsomkron P, Belin de Chantemele EJ, Mintz JD, Muta K, Salet C, et al. Deletion of protein tyrosine phosphatase 1b improves peripheral insulin resistance and vascular function in obese, leptin-resistant mice via reduced oxidant tone. Circ.Res. 2009;105:1013-22.

[42] Vercauteren M, Remy E, Devaux C, Dautreaux B, Henry JP, Bauer F, et al. Improvement of peripheral endothelial dysfunction by protein tyrosine phosphatase inhibitors in heart failure. Circulation 2006;114:2498-507.

[43] Fleming I, Bauersachs J, Fisslthaler B, Busse R. Ca2+-independent activation of the endothelial nitric oxide synthase in response to tyrosine phosphatase inhibitors and fluid shear stress. Circ.Res. 1998;82:686-95.

[44] Coquerel D, Neviere R, Delile E, Mulder P, Marechal X, Montaigne D, et al. Gene Deletion of Protein Tyrosine Phosphatase 1B Protects Against Sepsis-Induced Cardiovascular Dysfunction and Mortality. Arterioscler.Thromb.Vasc.Biol. 2014;34:1032-44.

[45] Galan M, Kassan M, Choi SK, Partyka M, Trebak M, Henrion D, et al. A novel role for epidermal growth factor receptor tyrosine kinase and its downstream endoplasmic reticulum stress in cardiac damage and microvascular dysfunction in type 1 diabetes mellitus. Hypertension. 2012;60:71-80.

[46] Kassan M, Galan M, Partyka M, Saifudeen Z, Henrion D, Trebak M, et al. Endoplasmic reticulum stress is involved in cardiac damage and vascular endothelial dysfunction in hypertensive mice. Arteriosclerosis, thrombosis, and vascular biology. 2012;32:1652-61.

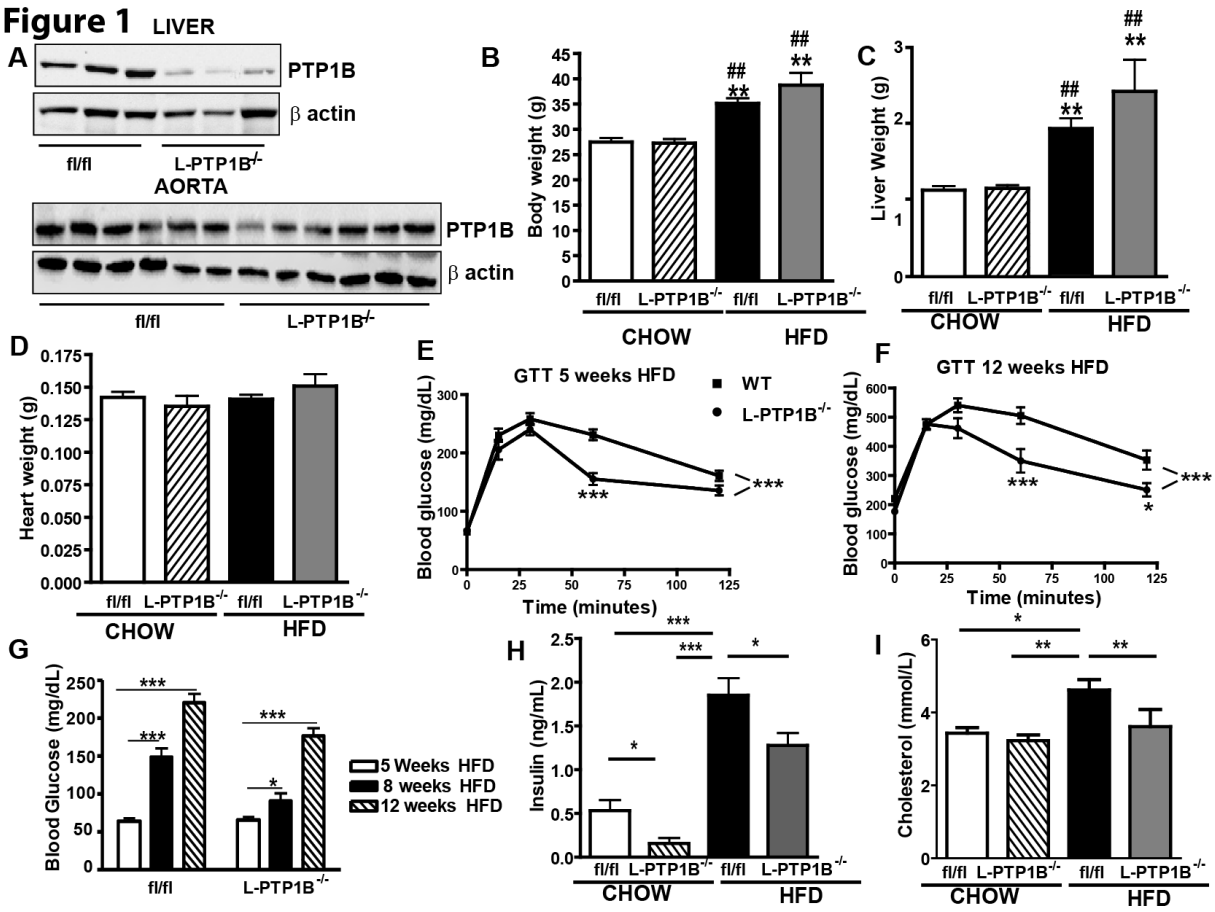
Figure 1 LIVER
A
PTP1B
β actin
fl/fl
L-PTP1B-/-
AORTA
PTP1B
β actin
fl/fl
L-PTP1B-/-
B
Body weight (g)
fl/fl L-PTP1B-/- fl/fl L-PTP1B-/-
CHOW
HFD
C
Liver Weight (g)
fl/fl L-PTP1B-/- fl/fl L-PTP1B-/-
CHOW
HFD
D
Heart weight (g)
fl/fl L-PTP1B-/- fl/fl L-PTP1B-/-
CHOW
HFD
E
GTT 5 weeks HFD
WT
L-PTP1B-/-
Blood glucose (mg/dL)
Time (minutes)
F
GTT 12 weeks HFD
Blood glucose (mg/dL)
Time (minutes)
G
Blood Glucose (mg/dL)
5 Weeks HFD
8 weeks HFD
12 weeks HFD
fl/fl
L-PTP1B-/-
H
Insulin (ng/mL)
fl/fl L-PTP1B-/- fl/fl L-PTP1B-/-
CHOW
HFD
I
Cholesterol (mmol/L)
fl/fl L-PTP1B-/- fl/fl L-PTP1B-/-
CHOW
HFD

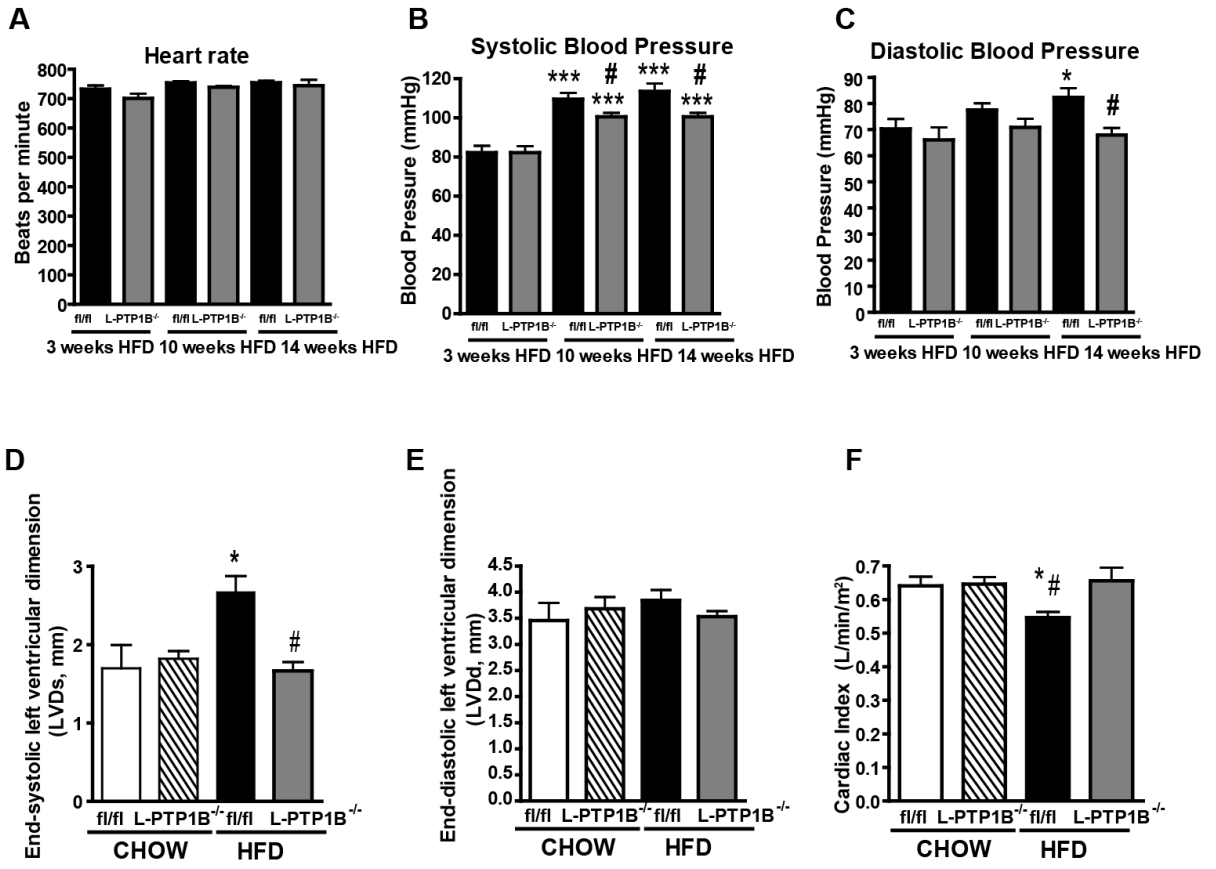
A
Heart rate
Beats per minute
800
700
600
500
400
300
200
100
0
fl/fl
L-PTP1B-/-
3 weeks HFD
10 weeks HFD
14 weeks HFD
B
Systolic Blood Pressure
Blood Pressure (mmHg)
120
100
80
60
40
20
0
***
#
C
Diastolic Blood Pressure
Blood Pressure (mmHg)
90
80
70
60
50
40
30
20
10
0
*
#
D
End-systolic left ventricular dimension (LVDs, mm)
3
2
1
0
*
#
CHOW
HFD
E
End-diastolic left ventricular dimension (LVDd, mm)
4.5
4.0
3.5
3.0
2.5
2.0
1.5
1.0
0.5
0.0
F
Cardiac Index (L/min/m²)
0.7
0.6
0.5
0.4
0.3
0.2
0.1
0.0
*#

Figure 2

Figure 3

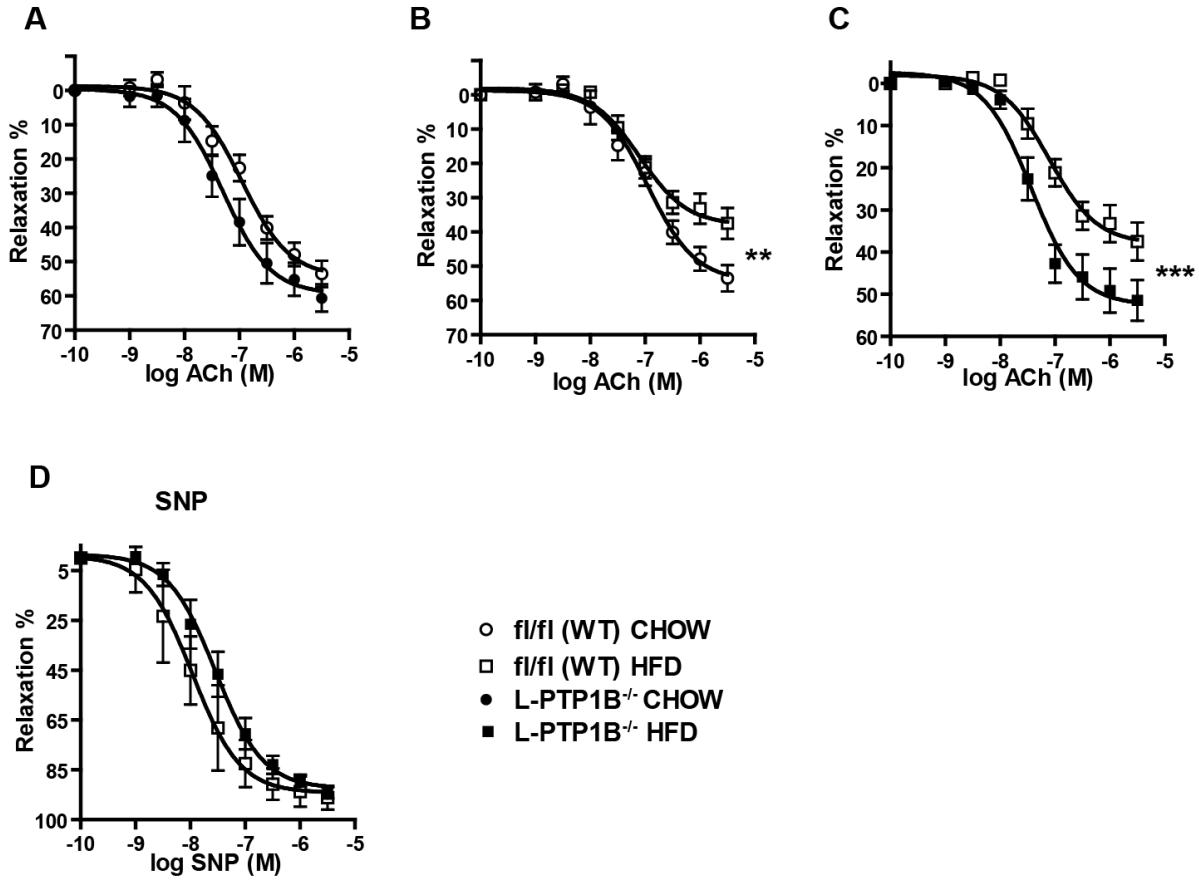
A
B
C
D
Relaxation %
log ACh (M)
log SNP (M)
SNP
**
***
fl/fl (WT) CHOW
fl/fl (WT) HFD
L-PTP1B-/- CHOW
L-PTP1B-/- HFD

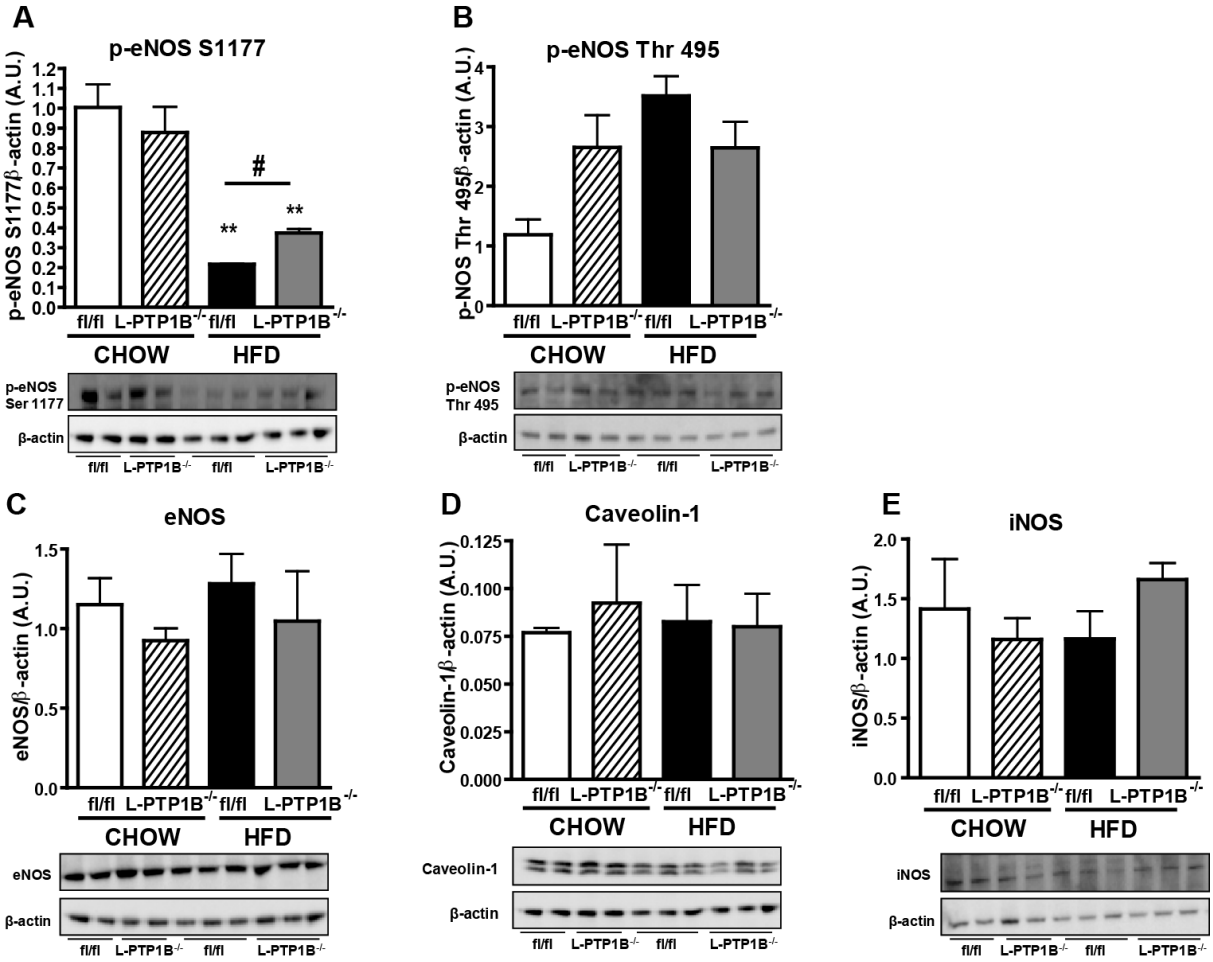
A
p-eNOS S1177
p-eNOS S1177/β-actin (A.U.)
1.2
1.1
1.0
0.9
0.8
0.7
0.6
0.5
0.4
0.3
0.2
0.1
0.0
#
**
**
fl/fl
L-PTP1B-/-
fl/fl
L-PTP1B-/-
CHOW
HFD
p-eNOS Ser 1177
β-actin
fl/fl
L-PTP1B-/-
fl/fl
L-PTP1B-/-
B
p-eNOS Thr 495
p-NOS Thr 495/β-actin (A.U.)
4
3
2
1
0
fl/fl
L-PTP1B-/-
fl/fl
L-PTP1B-/-
CHOW
HFD
p-eNOS Thr 495
β-actin
fl/fl
L-PTP1B-/-
fl/fl
L-PTP1B-/-
C
eNOS
eNOS/β-actin (A.U.)
1.5
1.0
0.5
0.0
fl/fl
L-PTP1B-/-
fl/fl
L-PTP1B-/-
CHOW
HFD
eNOS
β-actin
fl/fl
L-PTP1B-/-
fl/fl
L-PTP1B-/-
D
Caveolin-1
Caveolin-1/β-actin (A.U.)
0.125
0.100
0.075
0.050
0.025
0.000
fl/fl
L-PTP1B-/-
fl/fl
L-PTP1B-/-
CHOW
HFD
Caveolin-1
β-actin
fl/fl
L-PTP1B-/-
fl/fl
L-PTP1B-/-
E
iNOS
iNOS/β-actin (A.U.)
2.0
1.5
1.0
0.5
0.0
fl/fl
L-PTP1B-/-
fl/fl
L-PTP1B-/-
CHOW
HFD
iNOS
β-actin
fl/fl
L-PTP1B-/-
fl/fl
L-PTP1B-/-

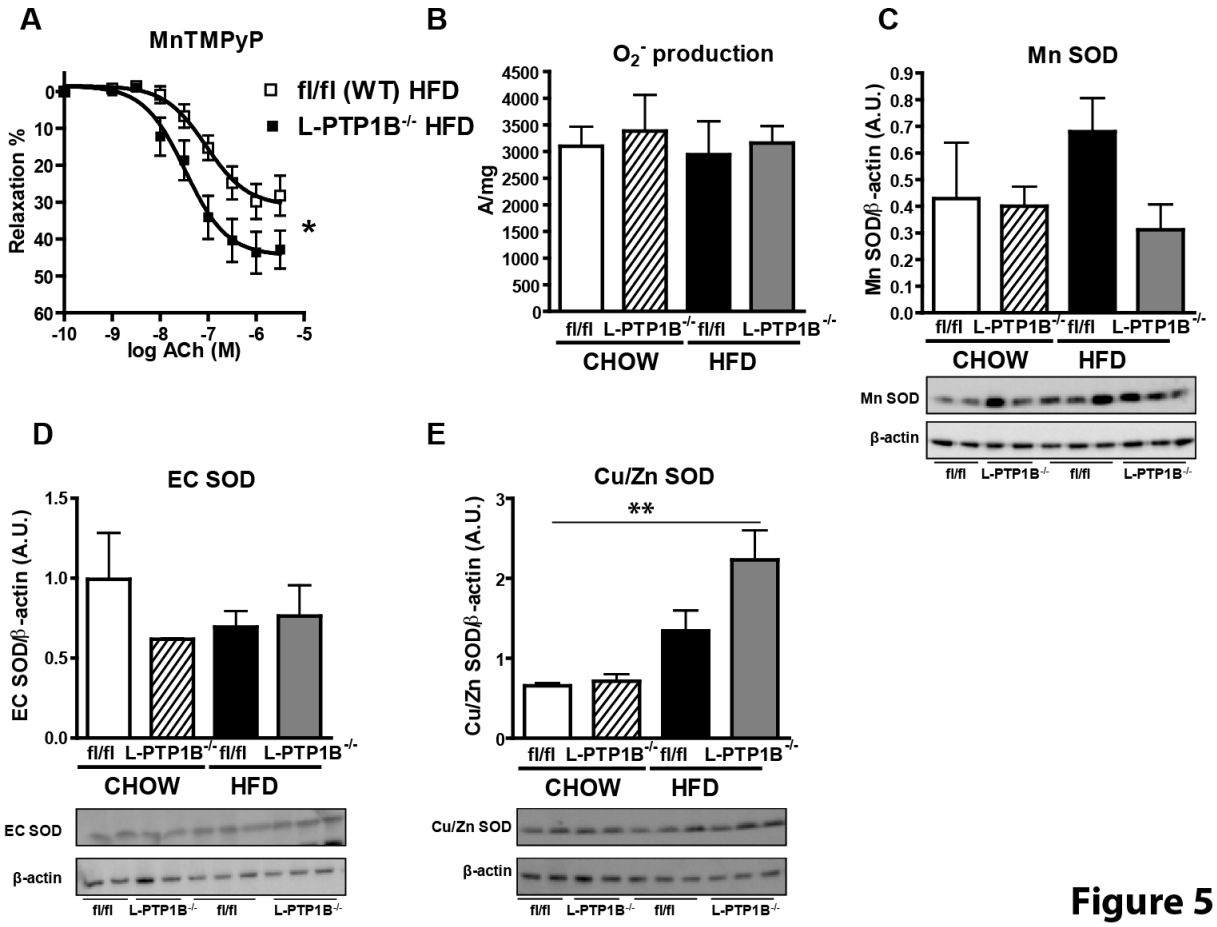
A
MnTMPyP
fl/fl (WT) HFD
L-PTP1B-/- HFD
Relaxation %
log ACh (M)
*
B
O2- production
A/mg
fl/fl L-PTP1B-/- fl/fl L-PTP1B-/-
CHOW HFD
C
Mn SOD
Mn SOD/β-actin (A.U.)
fl/fl L-PTP1B-/- fl/fl L-PTP1B-/-
CHOW HFD
Mn SOD
β-actin
fl/fl L-PTP1B-/- fl/fl L-PTP1B-/-
D
EC SOD
EC SOD/β-actin (A.U.)
fl/fl L-PTP1B-/- fl/fl L-PTP1B-/-
CHOW HFD
EC SOD
β-actin
fl/fl L-PTP1B-/- fl/fl L-PTP1B-/-
E
Cu/Zn SOD
**
Cu/Zn SOD/β-actin (A.U.)
fl/fl L-PTP1B-/- fl/fl L-PTP1B-/-
CHOW HFD
Cu/Zn SOD
β-actin
fl/fl L-PTP1B-/- fl/fl L-PTP1B-/-

Figure 5

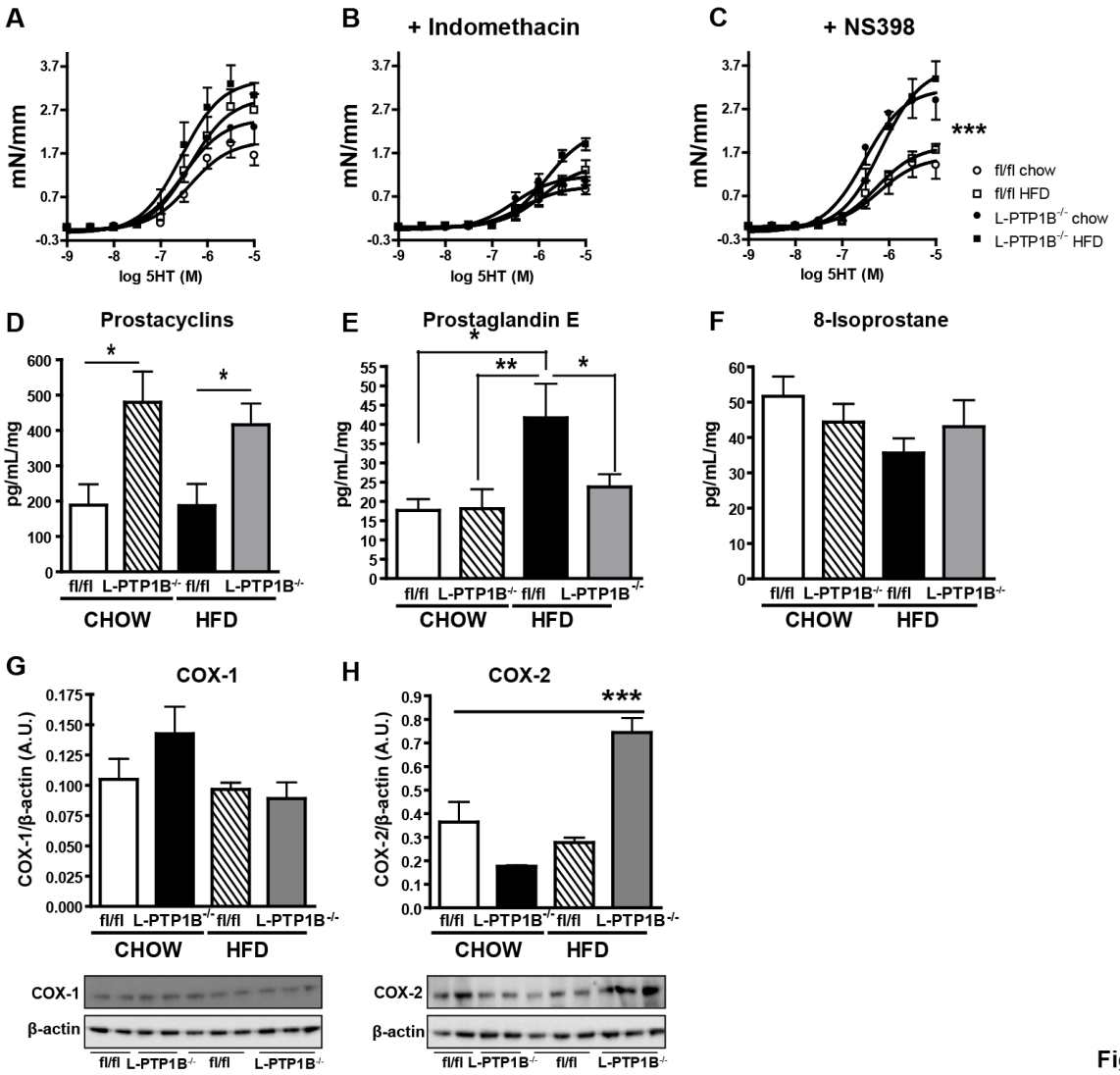
A
B
+ Indomethacin
C
+ NS398
mN/mm
log 5HT (M)
***
fl/fl chow
fl/fl HFD
L-PTP1B-/- chow
L-PTP1B-/- HFD
D
Prostacyclins
pg/mL/mg
E
Prostaglandin E
F
8-Isoprostane
fl/fl
L-PTP1B-/-
CHOW
HFD
G
COX-1
COX-1/β-actin (A.U.)
H
COX-2
COX-2/β-actin (A.U.)
β-actin

Figure 6

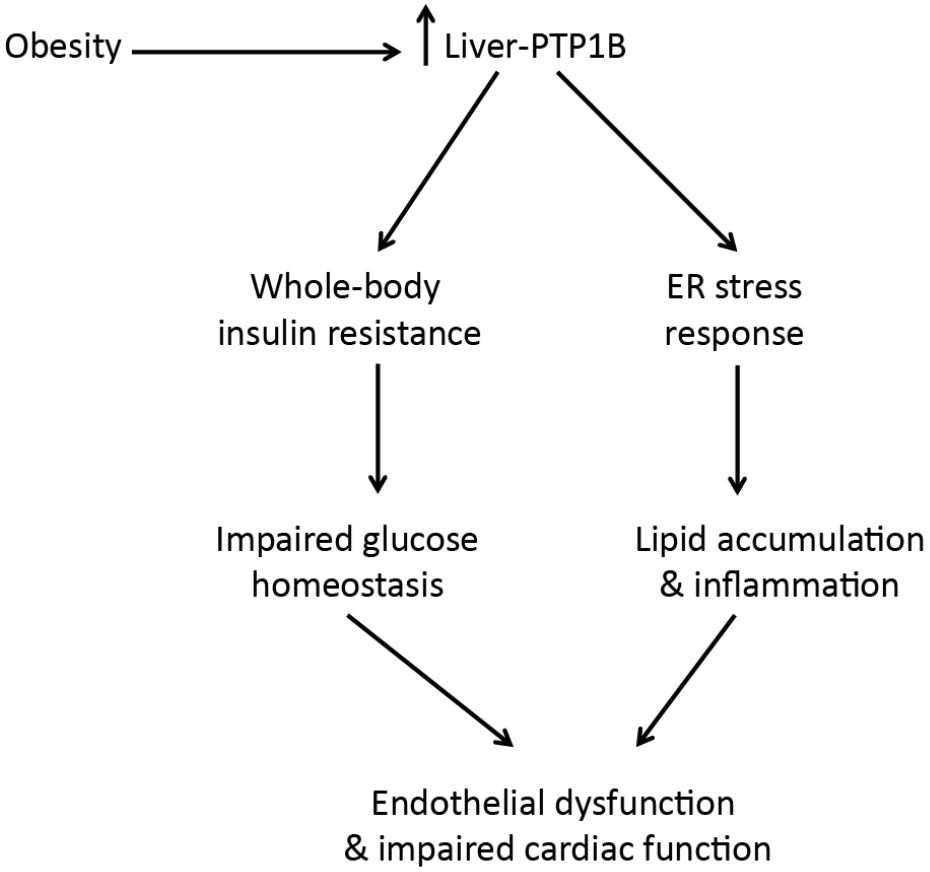
Obesity
Liver-PTP1B
Whole-body
insulin resistance
ER stress
response
Impaired glucose
homeostasis
Lipid accumulation
& inflammation
Endothelial dysfunction
& impaired cardiac function

Figure 7